A Divisive Inhibition Model for Chromoluminance Pattern Equidiscrimination Contours

Chien-Chung Chen[a], John M. Foley[b], & David H. Brainard[b]
[a]Smith-Kettlewell Eye Research Institute, San Francisco, CA
[b]Psychology Department, University of California, Santa Barbara, CA

ABSTRACT

We studied the detection of chromoluminance patterns in the presence of chromoluminance pedestals. We examined how thresholds depend on the color directions of the target and the pedestal. Both targets and pedestals were spatial Gabor patterns (horizontal, 1 cpd) . The patterns were spatially modulated in color, luminance or both. Equidiscrimination contours describe contrast thresholds for targets in different color directions on the same pedestal. We measured the equidiscrimination contours on green/red and blue/yellow pedestals. The equidiscrimination contours are asymmetrically related to the cardinal axes in isoluminant plane. The shape of the equidiscrimination contours changes with the contrast and the color directions of the pedestals. We applied a model with three pairs of mechanisms that we proposed earlier[6] to these data. Each mechanism consists of a linear receptive-field like color-spatial operator followed by a nonlinear process. The nonlinear process takes two inputs: the excitation comes directly from the linear operator and the divisive inhibition is a nonlinear sum of all linear operator responses. Two linear operator pairs are color opponent while the third is non-opponent. The detection variable is computed from the outputs of the nonlinear processes combined by Quick's pooling rule.

Keywords: chromoluminance, masking, chromatic pattern vision model, divisive inhibition.

1. INTRODUCTION

In most natural images both the intensity and the spectral composition of light vary over space. Such modulation of light across space can be analyzed into the sum of a luminance (isochromatic) modulation and a chromatic (isoluminant) modulation. Luminance modulations carry a large amount of information about spatial structure, but the information carried by the chromatic modulation can also be important.[4,7] Thus, to fully understand the way the human visual system works, it is important to know how the visual system responds to both luminance and chromatic modulations in images. However, spatial vision and color vision are often studied separately using different kinds of stimuli and methods. For instance, spatial vision research often uses periodic patterns modulated in luminance while color vision research focuses on homogeneous fields and spots. As a result, there is a substantial body of measurements and models relating to the visual processing of luminance patterns[9,18,52] or chromatic spots.[56] There is a less extensive body of research on chromatic pattern vision and less still on patterns that combine luminance and chromatic modulation, though there is a growing interest in this.[7,17,30,31,34,35,40,41,42,44,46,51] The primary goal of this study is to extend our knowledge of chromoluminance pattern vision. We use the term chromoluminance pattern to refer to a spatial modulation in either luminance, chromaticity, or both. In this paper, our focus is on patterns that vary in chromaticity.

Our project has two components. First, we studied the performance of the visual system in detecting chromoluminance patterns empirically with psychophysical experiments. Second, we proposed and tested a quantitative model for chromoluminance pattern vision. The psychophysical experiments measure the contrast detection threshold of a target chromoluminance pattern superimposed on a pedestal that is also a chromoluminance pattern. This simultaneous superimposed masking paradigm has been used to develop quantitative models of the mechanisms that encode information about spatial pattern.[16,29,43,50,53] An advantage of the masking paradigm is that it can be used to measure effects over a large range of pedestal contrasts and thus can provide information about the response properties of the visual system over this range. Also, by systematically varying the pedestal along a dimension, the simultaneous superimposed masking paradigm provides a way to observe how the visual system responds to that dimension and how mechanisms that respond to the pedestal interact with the mechanisms that respond to the target if they should be different. To date, there have been only a few pattern masking studies that have used isoluminant stimuli.[8,30,35,46] The purpose of these studies was primarily to investigate the interaction between luminance and chromatic patterns, and the stimuli were limited to patterns modulated along green-red and yellow-black directions in color space. Our study provides contrast threshold measurements for many chromoluminance targets presented on many chromoluminance pedestals. We have previously reported data for the target threshold vs. pedestal contrast (TvC) functions for five chromoluminance targets on 13 chromoluminance pedestals[5]. Those data provide rich information about the response characteristics of the visual system to chromoluminance patterns. Here, we

Part of the IS&T/SPIE Conference on Human Vision
and Electronic Imaging IV • San Jose, California • January 1999
SPIE Vol. 3644 • 0277-786X/99/$10.00

present data for 16 isoluminance targets on two isoluminance pedestals and show how contrast thresholds change with target color directions on different pedestal color directions and contrasts.

Our modeling effort has been focused on two issues. The first one concerns the response characteristics of the chromoluminance pattern vision mechanisms. From the studies of isochromatic luminance pattern vision, there is considerable evidence that nonlinear excitatory and divisive-inhibitory processes mediate the visual system's response to luminance patterns.[1,16,21] Does the visual system's response to chromoluminance patterns in general share the same non-linearity? The second issue concerns the spectral properties of the chromoluminance pattern vision mechanisms. Current estimates of the spectral properties of the post-receptoral visual mechanisms[19,20,24] are based on psychophysical experiments with spots or homogeneous fields. These stimuli do not stimulate pattern vision mechanisms well.[9,23,52] Thus, it is reasonable to wonder if the chromoluminance pattern mechanisms have same spectral sensitivities.

2. PSYCHOPHYSICAL EXPERIMENT

2.1 Methods

Our methods are described in detail elsewhere[5]. Here is a summary.

2.1.1 Stimuli

Patterns were presented in a rectangular field (5°V x 7°H) and viewed from a distance of 162 cm. There was a small dark fixation point in the center of the field. Both targets and pedestals were horizontal Gabor patterns with a center spatial frequency of 1 c/deg. The scale parameter (standard deviation) of the Gaussian spatial envelope was 1 degree in both horizontal and vertical directions. The patterns were modulated in cosine phase relative to the fixation point and to the peak of the envelope. All modulations were around a single white point with CIE xy chromaticity (0.28, 0.31) and luminance 29.6 cd/m^2. The background was this same white and was on continuously. All stimuli were presented using a truncated Gaussian temporal waveform with a scale parameter of 40 ms and a total duration of 160 msec. Target and pedestal were always coincident in time and superimposed in space.

The chromatic modulation of the targets and pedestals was always along a straight line in cone excitation space. Such a modulation can be represented by a vector in cone contrast space.[3] The L-cone contrast of the pattern, C_L, is defined as $\Delta L/L_0$ where L_0 is the L-cone excitation produced by the background and $\Delta L=L-L_0$ is the L-cone excitation deviation at the central point of the pattern. If there is a decrement in cone excitation at the central point, then the cone contrast is negative. The M-cone and S-cone contrasts, C_M and C_S, are defined similarly and the chromoluminance modulation is given by the vector $\underline{C}=[C_L, C_M, C_S]^T$. Note that, if the phase of the underlying sinewave is shifted by 180 degrees, the direction of the vector reverses. Cone contrasts are calculated using the Smith-Pokorny estimates of the cone spectral sensitivities.[10,45] It is convenient to specify modulations in terms of their contrast and color direction. Color direction is given by the normalized vector, $\underline{C}/\|\underline{C}\|$. There are a number of different measures that have been used to specify contrast across different color directions. Here we define the contrast of a modulation as:

$$\underline{C}= (C_L^2+C_M^2+C_S^2)^{0.5} / (3)^{0.5}. \quad (1)$$

This measure is proportional to the square root of cone contrast energy and varies between 0 and 1, the same range as Michelson contrast. Although we use this definition to describe our stimuli and results, we do not draw conclusions that depend on the comparison of contrast across modulation color directions.

A cone contrast vector $\underline{C}$ is defined as a linear combination of contrast vectors in the three cardinal color directions[11,27,33]. Table 1 provides a descriptive name and the L, M, and S cone contrasts for each of the cardinal directions. An arbitrary cone contrast vector is defined as

$$\underline{C} = \cos(\phi)\cos(\theta)\,\underline{BY} + \sin(\phi)\cos(\theta)\,\underline{GR} + \sin(\theta)\,\underline{LUM} \quad (2)$$

where $\underline{BY}$, $\underline{GR}$, and $\underline{LUM}$ are normalized vectors on cardinal directions as described in Table 1 and θ and ϕ are angles between $\underline{C}$ and $\underline{BY}$ toward $\underline{LUM}$ and $\underline{GR}$ respectively. We will refer to $\underline{LUM}$ as isochromatic because it does not vary in chromaticity. We will refer to stimuli on a plane spanned by $\underline{BY}$ and $\underline{GR}$ (i.e., θ=0) as

Table 1. Cardinal color directions

Descriptive Name	Cone contrast coordinate	Symbol
Isochromatic	(1, 1, 1)	LUM
Green/red	(-0.8413, 0.5140, 0)	GR
Blue/yellow	(0, 0, 1.732)	BY

nominally isoluminant because they are orthogonal to the Judd-Vos photopic luminosity function[47] V_λ.

In contrast with other studies of pedestal effects with chromoluminance patterns, in our experiment we did not tailor our stimuli to the subjective isoluminant plane of the individual observers. The term subjective isoluminant plane refers to the isoluminant plane defined for an individual observer by flicker photometry or a related technique. We have chosen instead to define isoluminance by the Judd-Vos photopic luminosity function[47] V_λ and to use the same set of nominally isoluminant stimuli for all our observers in our main experiment. Our nominal isoluminant stimuli lie on a plane in the color space that is orthogonal to the direction defined by the V_λ function. Except where stated otherwise, the term isoluminance in this paper refers to nominal isoluminance rather than subjective isoluminance determined psychophysically for individual observers

2.1.2 Equipment

Target and pedestal patterns were presented on separate color monitors (Sony CPD-1730) each driven by its own graphics board (RasterOps Turbo XL). Each graphics board provided 9 bits of intensity resolution in each color channel. A single host computer (Macintosh IIfx) controlled the two graphics boards. The output of the two monitors was optically combined by a beam-splitter. We used two beam splitters with different transmission ratios in different conditions as a means of adjusting the contrast range of our stimuli. Refresh timing of the two monitors was synchronized with custom software, and target and pedestal contrasts could be varied simultaneously during a single vertical blanking period. The frame rate of the monitors was 75 Hz. The monitors had a spatial resolution of 832 horizontal by 624 vertical pixels. At the distance we used (162 cm), there were 76 pixels per grating cycle.

2.1.3 Procedure

To measure contrast threshold, we used a temporal two-alternative forced choice procedure in which the pedestal alone was presented in one interval and the target and pedestal superimposed were presented in the other interval. The interstimulus interval was 480 msec. Target contrast for each trial was chosen using the Quest adaptive procedure.[37, 49]

2.1.4 Experimental Design

There were 16 isoluminant targets used in this experiments. There were 2 chromoluminance pedestals with different combination of chromatic and luminance contrast. There were 32 target-pedestal pairs used. We measured target contrast on 2 pedestal contrasts for each target-pedestal pair. We also measured the absolute contrast threshold for each target (the threshold at 0 pedestal contrast). Reported thresholds are the mean of four or six individual measurements made in separate sessions.

2.1.5 Observers

There were two principal observers for TvC functions reported previously[5], one of the authors (CCC, male in his late twenties) and one naive observer (JKL, female in her early twenties). Another observer (JMF, male in his late fifties) participated experiments with green/red and blue/yellow targets. The equidiscrimination contours that are the focus measured in this paper were measured only for CCC. All observers had normal (20/20) or corrected to normal visual acuity and normal color vision as tested with the Ishihara plates.[25] All the observers had at least several hours of practice before the experiment began.

2.2 Experimental results

2.2.1 Target-threshold vs. pedestal contrast (TvC) functions

A pedestal can have very different effects on target detection as its contrast is varied. At one contrast a pedestal can decrease target threshold while at another contrast it can increase threshold. Also, different pedestals may have dramatically different effects on the same target. Data shown in Fig. 1, taken from the earlier study[5], illustrate this. In this figure, we show the Target-threshold vs. pedestal contrast (TvC) functions for one green/red target on three different pedestals. In general, the shape of TvC functions varies with both the target and the pedestal.[16,44] A detailed treatment of the TvC functions can be found elsewhere.[5] Here we give an example of how thresholds for one target can vary with pedestal color direction and contrast.

Fig. 1 shows the TvC functions for the green/red target on pedestals modulated along cardinal axes (i.e., isochromatic, green/red and blue/yellow). When detecting a green/red target on a green/red pedestal, the threshold first decreases from the absolute threshold (facilitation) and then increases above the absolute threshold (masking) as pedestal contrast increases. The maximum facilitation occurs at around the pedestal absolute threshold. This "dipper" shape TvC function is commonly found in luminance pattern masking literature. The blue/yellow pedestal does not facilitate green/red target detection but it does mask the green/red target. Notice that the lowest blue/yellow pedestal contrast is already about 12 dB lower than its absolute threshold (or only 25 % of the absolute threshold). The isochromatic pedestal facilitates the green/red target over a wide range of pedestal contrast and the maximum facilitation occurs at a pedestal contrast that is about 10 times higher than the pedestal absolute threshold. This figure illustrates that the shapes of the TvC functions can vary substantially as a function of the pedestal color direction.

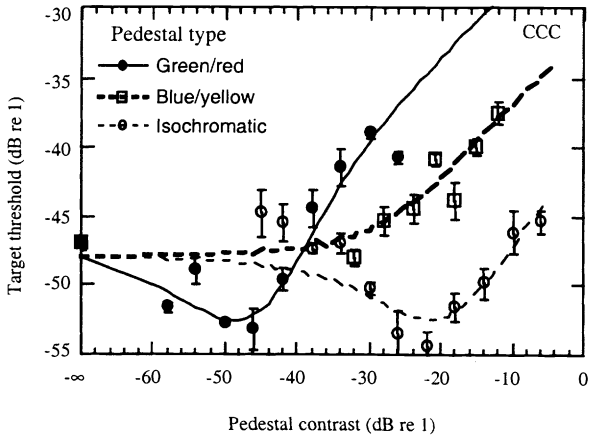

Fig1. TvC functions for green/red targets. In this and the rest figures in this paper, the smooth curves are model fits. The closed circles and the continuous curve are for green/red pedestal. The open squares and the bold dashed curve are for blue/yellow pedestal. The open circles and the light dashed curves are for isochromatic pedestal. The error bars are standard error of measurements. In this and other data figures, the smooth curves are fits of the model discussed in the text.

2.2.2 Equidiscrimination contour on the green/red pedestal

The data can also be organized as the thresholds of various targets on a pedestal with a single color direction and contrast. The combination of the pedestal and targets at these thresholds are equally discriminable from the pedestal itself. This is a approach commonly used in color discrimination literature.[26,28,32,36,38,55] Fig. 2 shows equidiscrimination contours on green/red isoluminance pedestals. In this figure, each point is plotted in a polar coordinate. The angle of each point to the blue/yellow axis is the angle ϕ defined in Eq. (2). We set the central point as –55 dB contrast for every color direction. Thus, The distance of each point to the central point is the detection threshold in dB unit minus -55. Notice that all contrasts are presented in dB (or 20 times log unit) in this paper.

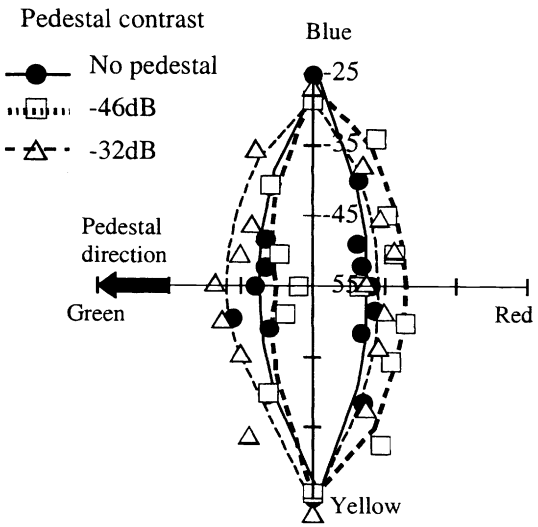

Fig. 2. Equidiscrimination contour on green/red pedestals. The closed circles and the continuous curves are for threshold contour with no pedestal. The open squares and the bold dotted curve are for –46 dB pedestal and the open triangles and the dash curves are for –32 dB pedestal. The bold arrow on the left denotes the direction of pedestal modulation. The thresholds are in dB units.

When there is no pedestal, the contour actually represents pattern detection threshold in each designated color direction. The contour has an elliptic shape, in general agreement with previous studies.[13,39] The shape of equidiscrimination contour changes when a pedestal is presented. At low pedestal contrast (-46 dB), the targets in the second and the third quadrants have their green/red component in phase with the pedestal. The green/red pedestal has a facilitative effect on those targets. Thus, in comparison to the contour with no pedestal, the equidiscrimination contour is compressed toward the central reference point. On the other hand, the targets at the first and the fourth quadrants have their green/red component 180-degree out-of-phase from the pedestal. The –46 dB pedestal has a masking effect on these targets. Thus, the equidiscrimination contour is pushed away from the reference point in these two quadrants. The contour no longer has an elliptic shape with respect to the central point. The –32dB pedestal has a strong masking effect on targets in the second and the third quadrants and pushes the equidiscrimination contour away from the reference point. This pedestal, however, has little masking effect on targets at the first and the fourth quadrants. Thus, in

these quadrants, the equidiscrimination contour is compressed from the –46 dB contour toward the reference point and closer to the contour with no pedestal.

2.2.3 Equidiscrimination contour on the blue/yellow pedestal

Fig. 3 shows the equidiscrimination contours on the blue/yellow pedestals. The change of contours with pedestal contrast is quite different from that for green/red pedestal. The blue/yellow pedestal has only masking effects on other isoluminant targets. The masking effect increases with pedestal contrast. As a result, the equidiscrimination contours expand further away with pedestal contrast. Notice that a -10 dB pedestal has a stronger masking effect on targets in the second and the third quadrants than those in the first and the fourth quadrants. This asymmetric effect suggests that the blue/yellow pedestal has different effects on the mechanisms that detect green/red and red/green targets.

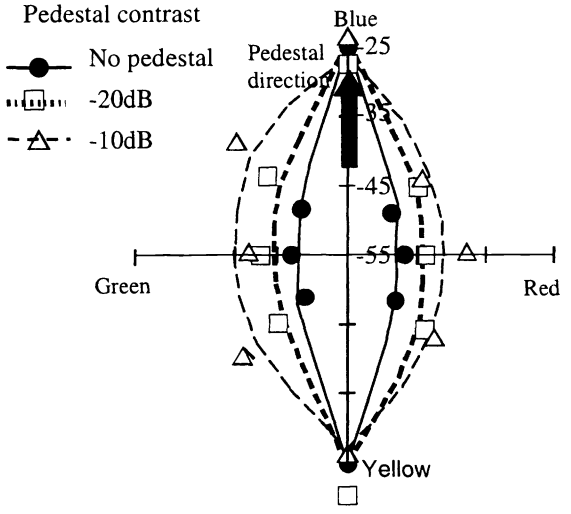

Fig. 3. Equidiscrimination contour on blue/yellow pedestals. The closed circles and the continuous curves are for threshold contour with no pedestal. The open squares and the bold dotted curve are for –20 dB pedestal and the open triangles and the dash curves are for –10 dB pedestal. The bold arrow on the left denotes the direction of pedestal modulation.

3. THE MODEL

We proposed a model for our earlier measurements of chromoluminance TvC functions based on five target color directions[6]. Here, we are interesting in whether the same model can extend to account for a wider range of target color directions. Since our focus is on the nature of the mechanisms and processes involved in chromoluminance pattern vision, we have included in our model only those mechanisms needed to account for our results, which are limited to one spatial frequency (1 c/deg), one orientation (horizontal), one phase relative to the fixation point (cosine) and one retinal position (centered on the fovea). It is clear from the literature on pattern vision that to account for detection and discrimination of patterns that differ from ours in spatial frequency, orientation, phase and position many more mechanisms will be needed.[53]

3.1 Model description

A schematic illustration of our model is shown in Fig. 4. This model has three pairs of mechanisms, each of which has four stages. The outputs of the mechanisms are combined into a single detection variable that determines the predicted threshold. The first stage of a mechanism is a chromoluminance linear operator. A linear operator takes input from each of the three cone arrays. For the periodic patterns as we used in our experiment, the output of the linear operator (net excitation) may be computed as weighted sum of the stimulus cone contrast. The six linear operators (and their corresponding mechanisms) are grouped into three opposite-sign pairs. Within each pair, the sensitivity of one member is simply the negative of the sensitivity of the other. Such paired mechanisms are required to account for pattern discrimination when the spatial phase between target and pedestal differs.[15] The asymmetric equidiscrimination contours we found also suggested the existence such opposite-sign pairs.

The excitation of each linear operator is half-wave rectified to produce *rectified excitation*. The output of a linear operator can be positive or negative. It is known that neurons in striate cortex, which are essential to pattern vision, have little maintained discharge. Thus, a linear operator does not by itself provide a biologically feasible model for cortical neurons. To increase the biological feasibility of our model, we follow each linear operator by half-wave rectification. The rectified excitation of j-th mechanism is denoted as Ej (+ and -) in Fig. 4.

For each mechanism, there is a *divisive inhibitory signal*. This signal is a nonlinear combination of the six rectified excitations. The divisive inhibition signals are identical within an opposite-sign pair but differ between mechanism pairs. The divisive inhibition signal to the j-th pair of mechanism is denoted as I_j (+ and -) in Fig 4.

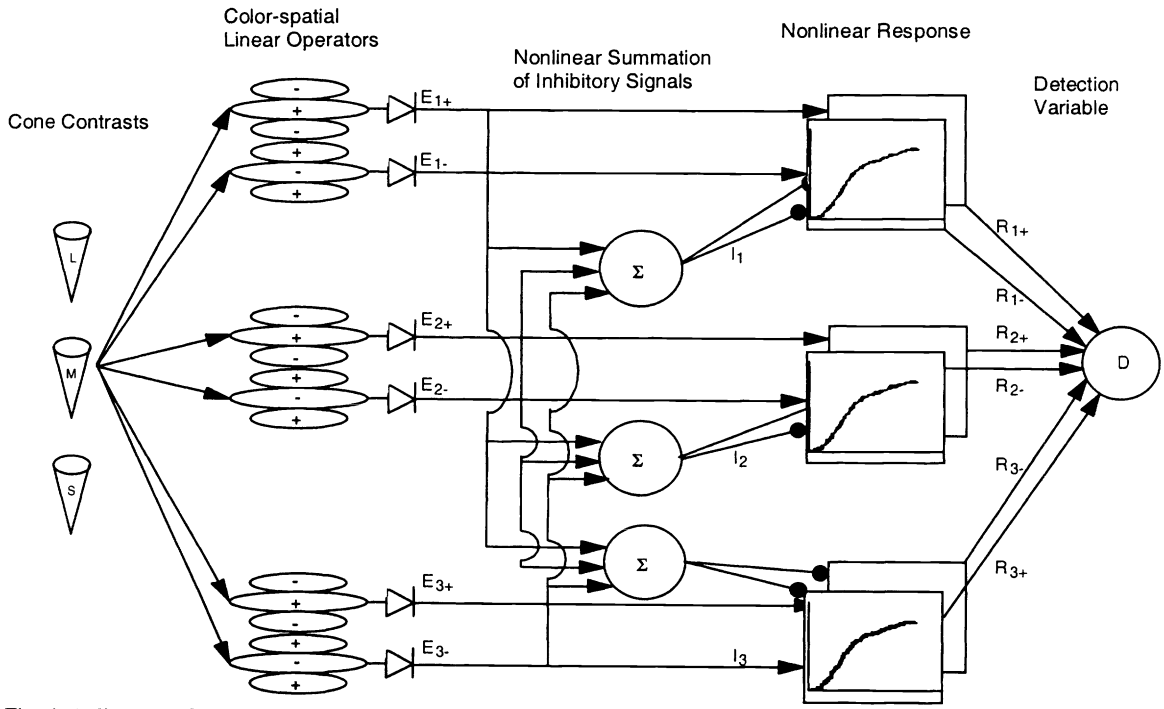

Fig. 4. A diagram of the divisive inhibition model for chromoluminance pattern masking.

The *mechanism response* is computed as the rectified excitation raised to a power and divided by a divisive inhibitory input plus a constant. The two mechanisms in each pair are identical except that their cone inputs are opposite in sign. The response of the j-th mechanism R_j (+ and -) is

$$R_j = E_j^p / (I_j + z) \qquad (3)$$

where p and z are constants.

To predict threshold in a two-alternative forced-choice pattern discrimination experiment, the six mechanism responses are computed for the pedestal plus target and pedestal alone. The absolute value of this difference is taken for each mechanism. These absolute differences are then weighted and summed nonlinearly to yield the *detection variable*. When target contrast is such that this variable exceeds unity, the target is above threshold. Threshold is then taken as the lowest target contrast where the detection variable is unity.

3.2 Performance of the Model

The smooth curves in Figure 1 to 3 are best fits of the model to the data. For each observer, all data points were fit with the same set of parameters. In our earlier work, where only the TvC function data were available, this model fitted the TvC function data reasonably well. The root mean square errors (RMSE) are 1.57 dB for CCC (335 data points), 1.41 dB for JKL (284 data points) and 1.09 dB for JMF (84 data points). These fit errors can be compared to the mean standard error of measurement: 0.77 dB for CCC, 0.73 dB for JKL and 0.72 dB for JMF. Because of the computing power limitations, we could not fit TvC and equidiscrimination data simultaneously. Instead, We used a procedure where first we fit the TvC data, then used the resulting parameters as the starting point for a fit to the equidiscrimination data. By iterating these two steps, we were able to fit both data set with similar parameter values. The final parameters were obtained by averaging those found by

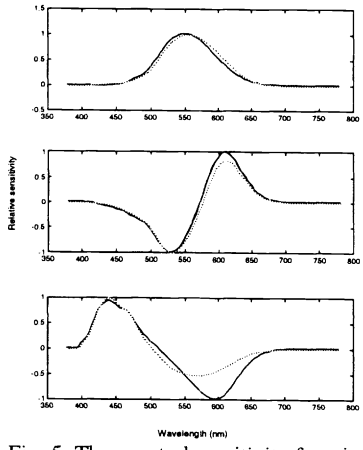

Fig. 5. The spectral sensitivity function of linear operators as estimated from the divisive inhibition model. See text for details.

the final two steps of iteration. These parameters gave a reasonable fits to the entire data set (observer CCC only) with an RMSE of 1.91 dB (comparing to 1.57 dB for the TvC function only. The smooth curves in Fig. 1-3 correspond to the combined fit. A better fit might have been obtained if it has been possible to fit entire data set simultaneously.

3.3 The spectral sensitivity of the linear operators

The spectral sensitivity functions of the linear operators can be estimated from the model parameters for sensitivity to cone. Since it is customary to describe color mechanisms in terms of their sensitivity to light (spectral sensitivity) rather than their sensitivity to contrast we transformed contrast sensitivity to spectral sensitivity.

The spectral sensitivity function of a linear operator is the inner product its cone spectral sensitivity and Smith-Pokorny cone fundamentals.[10,45] Fig. 5 shows the spectral sensitivity functions of the three linear operators derived from observer CCC's data. Each spectral sensitivity function is normalized by its peak value. The continuous curve shows the model estimation of three of the spectral sensitivity functions and the dotted curves are the Vos-Judd V_λ function[46] (panel A), the green/red mechanism (proposed by Guth et al.[20], panel B), and the yellow/blue mechanism proposed by Guth et al. [20] (panel C). The other three model sensitivity curves are the same except the signs are opposite. Qualitatively, our derived estimations agree with the mechanisms derived from these other studies. One operator can be identified with a luminance mechanism, one with a green/red mechanism and with a blue/yellow mechanism. The other three are an opposite-phase luminance mechanism, a red/green mechanism (excited by red in the center) and a yellow/blue mechanism.

4. DISCUSSION

We are aware of no other models that directly address chromoluminance pattern detection and discrimination. Nonetheless, it is possible to extend extant models so that they make predictions for pedestal effects on the detection of chromoluminance patterns, and to compare their performance with that of our model. We show that these simpler models make qualitative errors in predicting our experimental results. The fits produced by the various models are illustrated by showing equidiscrimination contours on green/red pedestals. In each case the model was fitted to the entire data set. The predictions of those models to TvC functions are discussed elsewhere.[6]

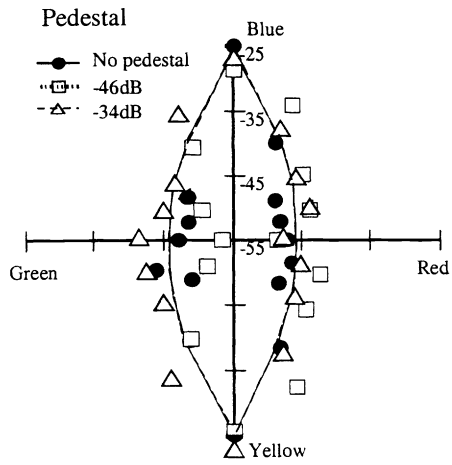

Fig. 6. Six-mechanism linear model predictions on equidiscrimination contours (cf. Fig. 3).

4.1 Linear models fail to predict our data

The two-stage color opponent model of Hurvich & Jameson[24] is a linear model in the sense that the outputs of the linear operators feed directly into a detection variable without intervening nonlinearities. Line-element theories[22,28,48] are also linear models in this sense, since the only nonlinearity in these theories is in the rule that pools the output of multiple mechanisms.

First consider a single mechanism version of such a linear model. This model predicts that threshold is reached when target contrast modulates the mechanism response (either up or down) by a fixed criterion amount. Whatever the pedestal, the effect of the target will be the same linear function of target contrast. Thus, this model predicts that the target threshold is independent of pedestal color direction and pedestal contrast and is therefore constant for each target in our experiment. Thus, the linear model predicts that the equidiscrimination contours at every pedestal contrast are the same ellipse. Clearly, the one mechanism linear model is qualitatively rejected by our data. We fitted a three-mechanism version of the linear model, The best fit of this model to the equidiscrimination contours for green/red pedestal in Fig. 6. The model

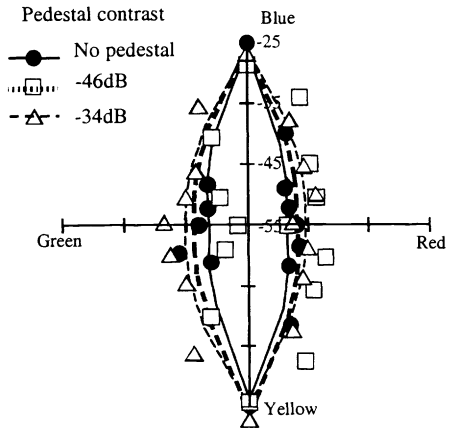

Fig. 7. Six-mechanism compressive nonlinear model predictions of equidiscrimination contours on green/red pedestals. (cf. Fig. 2)

clearly fails to account even roughly for the effects of the pedestals.

4.2 Simple exponential nonlinear response functions fail to predict our data

It appears that to account for facilitation and masking, a nonlinear process in the model is necessary. Fechner[14] suggested a compressive nonlinearity to explain the increase in discrimination thresholds as stimulus magnitude increases. This model predicts masking, but not facilitation. We fitted this model to our data and the best fit to the equidiscrimination contours on green/red pedestal, shown in Fig 7. Clearly the model fails to account for our data. The predicted contours expand away from the reference point as pedestal contrast increases. It is possible to substitute an expansive nonlinearity in place of compressive nonlinearity by setting the exponent of the response function being larger than 1. This model predicts facilitation, but not masking. Thus, a model with simple exponential nonlinearity predicts that the shapes of the equidiscrimination contours should either expand or shrink monotonically as the pedestal contrast increases. It cannot account for the shapes of our equidiscrimination contour, which has its left half shrink and then expand as pedestal contrast increases. This model is also inadequate. Substituting other forms of compressive and expansive nonlinearities will not overcome this weakness.

4.3 Static nonlinearity model fails to predict our data

More generally, one can consider models with arbitrarily complex static nonlinearities substituted for eq. 4. Legge and Foley[29] proposed such a model with an S-shaped nonlinearity, accelerating, then decelerating, as contrast increases. Wilson et al.[54] proposed a similar model. In the Legge and Foley model, the response function has the form (cf. Eq. 3):

$$R = E^p / (E^q+Z),$$

where E is the output of the linear operators and p, q, and Z are constants. This type of model predicts both facilitation and masking. But it does not provide a good quantitative fit to our data (see Fig. 8). The model predicts both facilitation and masking much smaller than our data show. We show elsewhere[6] that the static nonlinearity model is also unable to predict important qualitative features of our measured TvC functions.

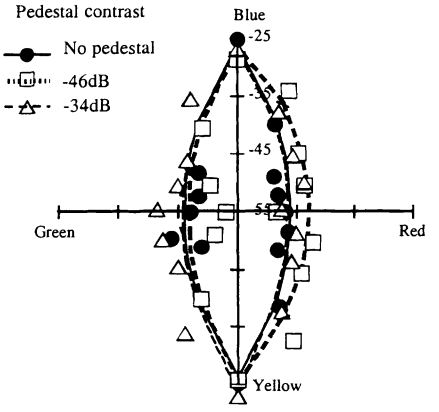

Fig. 8. Six-mechanism static nonlinear model predictions of equidiscrimination contours on green/red pedestals. (cf. Fig. 2)

4.4. The need of non-unity exponent in response functions

To account for contrast induction effects, D'Zmura[12] proposed a model that has 72 linear color-spatial filters followed by a nonlinear contrast normalization process. His model is similar to ours in many respects. The main difference is that the excitation is raised by a power of 1 (cf. Eq. 3). Could a model with this form of nonlinearity account for our data? Since this model assumes that the exponent to the linear operator excitation is 1, this model lacks the accelerating nonlinearity in the response function. As a result, it is impossible for a pedestal to facilitate target detection. Thus, this model can only predict masking, but not facilitation. Fig. 9 shows the predictions of this model. This model fails to capture the facilitation effect commonly observed in the data.

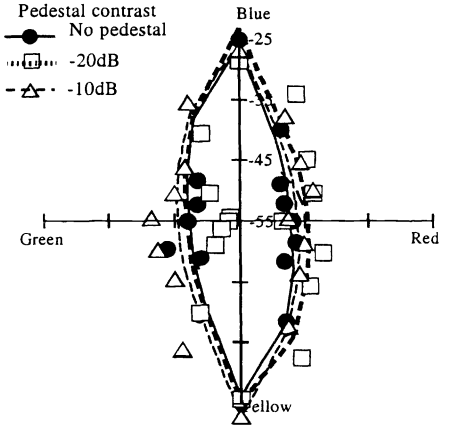

Fig 9. The prediction of D'Zmura's model for equidiscrimination contours on green/red pedestals. (cf. Fig. 2)

REFERENCES

1. Albrecht, D.G., & Geisler, W.S. (1991). Motion Sensitivity and the contrast-response function of simple cells in the visual cortex. *Visual Neuroscience*, **7**, 531-546.
2. Brainard, D.H. (1989). Calibration of a computer controlled color monitor. *Color Research and Application*, **14**, 23-34.
3. Brainard, D.H. (1996). Cone contrast and opponent modulation color spaces. In P.K. Kaiser & R.M. Boynton (Eds.), *Human Color Vision* . Washington D.C.: Optical Society of America.
4. Brill, M. H. Image segmentation by object color: a unifying framework and connection to color constancy. *Journal of the Optical Society of America A*, **7**, 2041-7.
5. Chen, C. C., Foley, J. M, & Brainard, D. H. (1999). Detection of Chromoluminance Patterns on Chromoluminance Pedestals I: Threshold Measurements. *Vision Research*. Submitted for review.
6. Chen, C. C., Foley, J. M, & Brainard, D. H. (1999). Detection of Chromoluminance Patterns on Chromoluminance Pedestals II: model. *Vision Research*. Submitted for review.
7. De Valois, K.K. (1994). *Spatial vision based on color differences*. Paper presented at the Computation vision based on neurobiology. SPIE Proceedings.
8. De Valois, K.K., & Switkes, E. (1983). Simultaneous masking interactions between chromatic and luminance gratings. *Journal of the Optical Society of America*, **73**,11-18.
9. De Valois, R.L., & De Valois, K.K. (1988). *Spatial Vision*. Oxford: Oxford University Press.
10. DeMarco, P., Pokorny, J., & Smith, V.C. (1992). Full-spectrum cone sensitivity functions for X-chromosome-linked anomalous trichromats. *Journal of the Optical Society A*, **9**, 1465-1476.
11. Derrington, A.M., Krauskopf, J., & Lennie, P. (1984). Chromatic mechanisms in lateral geniculate nucleus of macaque. *Journal of Physiology (London)*, **357**, 241-265.
12. D'Zmura, M. (1997). Color contrast gain control. In W. Backhaus, R. Kliegle, & J. Werner (Eds.), *Color Vision* . New York: Walter & Gruyter.
13. Elsner, A. E. Pokorny, J. & Burns, S. A. (1986). Chromaticity discrimination: effects of luminance contrast and spatial frequency, *Journal of the Optical Society of America A*, **3**, 916-20.
14. Fechner, G. (1859/1966). *Elements of Psychophysics*. (Adler, H. E., Trans.) NY: Holt.
15. Foley, J. M. & Chen, C. C. (1998) Pattern Detection in the Presence of Maskers that Differ in Spatial Phase and Temporal Offset: Threshold Measurements and a Model. *Vision Research,* (in press).
16. Foley, J.M. (1994). Human luminance pattern-vision mechanisms: Masking experiments require a new model. *Journal of the Optical Society of America A*, **11**, 1710-1719.
17. Gegenfurtner, K.R., & Kiper, D.C. (1992). Contrast detection in luminance and chromatic noise. *Journal of the Optical Society of America A*, **9**, 1880-1888.
18. Graham, N. (1988). *Visual Pattern Analyzer*. Oxford: Oxford University Press.
19. Guth, S.L. (1991). Model for color vision and light adaptation. *Journal of the Optical Society of America*, **8**, 976-993.
20. Guth, S.L., Massof, R.W., & Benzschawel, T. (1980). Vector model for normal and dichromatic color vision. *Journal of the Optical Society of America*, **70**, 197-212.
21. Heeger, D.J. (1992). Normalization of cell responses in cat striate cortex. *Visual Neuroscience*, **9**, 181-197.
22. Helmholtz, H. (1896/1962). *Treatise on Physiological Optics*. New York: Dover.
23. Hubel, D.H., & Wiesel, T.N. (1962). Receptive fields, binocular interaction and functional architecture in the cat's striate cortex. *Journal of Physiology*, **160**, 106-154.
24. Hurvich, L.M., & Jameson, D. (1957). An opponent-process theory of color vision. *Psychological Review.*, **64**, 384-404.
25. Ishihara, S. (1977). *Tests for Colour-Blindnes*. Tokyo: Kanehara Shuppen Company, Ltd.
26. Krauskopf, J., & Gegenfurtner, K. (1992). Color discrimination and adaptation. *Vision Research*, **32**, 2165-2175.
27. Krauskopf, J., Williams, D.R., & Heeley, D.W. (1982). Cardinal directions of color space. *Vision Research*, **22**, 1123-1131.
28. Le Grand, Y. (1949/1994). (Color difference thresholds in Young's theory). , *Color Research and Application,* **19**, 296-309.
29. Legge, G.E., & Foley, J.M. (1980). Contrast masking in human vision. *Journal of the Optical Society of America*, **70**, 1458-1470.
30. Losada, M.A., & Mullen, K.T. (1994). The spatial tuning of chromatic mechanisms identified by simultaneous masking. *Vision Research*, **34**, 331-341.
31. Losada, M.A., & Mullen, K.T. (1995). Color and luminance spatial tuning estimated by noise masking in the absence of off-frequency looking. *Journal of the Optical Society of America A*, **12**, 250-260.

32. MacAdam, D. L. (1942)Visual sensitivity to color difference in day light. *Journal of the Optical Society of America*, **32**, 247-274.
33. MacLeod, D.I.A., & Boynton, R.M. (1979). A chromaticity diagram showing cone excitation by stimuli of equal luminance. *Journal of the Optical Society of America*, **69**, 1183-1186.
34. Mullen, K.T., & Kingdom, F.A.A. (1991). Colour contrast in form perception. In P. Gouras (Ed.),, *The Perception of Colour* . Boca Raton: CRC Press.
35. Mullen, K.T., & Losada, M.A. (1994). Evidence for separate pathways for color and luminance detection mechanisms. *Journal of the Optical Society of America A*, **11**, 3136-3151.
36. Nagy A. L., Eskew R. T. & Boynton R. M. (1987). Analysis of color-matching ellipses in a cone-excitation space. *Journal of the Optical Society of America A*, **4**, 756-768.
37. Pelli, D.G., & Farrell, B. (1995). Psychophysical methods. In M. Bass (Ed.),, *Handbook of Optics: Volume 1. Fundamentals, Techniques, and Design* . New York: McGraw-Hill.
38. Poirson, A. B. & Wandell, B. A. (1990). Task dependent color discrimination. *Journal of the Optical Society of America A*, **10**, 2458-2470.
39. Poirson, A. B. , Wandell, B. A. , Varner, D. C. & Brainard, D. H. (1990). Surface characterizations of color thresholds. *Journal of the Optical Society of America A*, **7**, 783-789.
40. Poirson, A.B., & Wandell, B.A. (1993). Appearance of colored patterns: Pattern-color separability. *Journal of the Optical Society of America A*, **10**, 2458-2470.
41. Poirson, A.B., & Wandell, B.A. (1996). Pattern-color separable pathways predict sensitivity to simple colored patterns. *Vision Research*, **36**, 515-526.
42. Regan, D. (1991). Spatial vision for objects defined by colour contrast, binocluar disparity and motion parallax. In D. Regan (Ed.),, *Spatial Vision* . Boca Raton:
43. Ross, J., & Speed, H.D. (1991). Contrast adaptation and contrast masking in human vision. *Proc. R. Soc. London, Ser. B*, **246**, 61-69.
44. Sekiguichi, N., Williams, D., & Brainard, D. (1993). Efficiency in detection of isoluminant and isochromatic interference fringes. *Journal of the Optical Society of America A*, **10**, 2118-2133.
45. Smith, V.C., & Pokorny, J. (1975). Spectral sensitivity of the foveal cone photopigments between 400 and 500 nm. *Vision Research*, **15**, 161-171.
46. Switkes, E., Bradley, A., & De Valois, K.K. (1988). Contrast dependence and mechanisms of masking interactions among achromatic and luminance gratings. *Journal of the Optical Society of America A*, **2**, 62-71.
47. Vos, J.J. (1978). Colorimetric and photometric properties of a 2^{o} fundamental observer. *Color Research and Application*, **3**, 125-128.
48. Wandell, A.B. (1982). Measurement of small color difference. *Psychological Review*, **89**, 281-302.
49. Watson, A.B., & Pelli, D.G. (1983). Quest: A Baysian adaptive psychometric method. *Perception & Psychophysics*, **33**, 113-120.
50. Watson, A. B. & Solomon, J. (1997). Model of visual contrast gain control and pattern masking. Journal of the Optical Society of America *A*, **14**, 2379-2391
51. Webster, M.A., de Valois, K.K., & Switkes, E. (1990). Orientation and spatial-frequency discrimination for luminance and chromatic gratings. *Journal of the Optical Society of America A*, **7**, 1034-1049.
52. Wilson, H. R. (1978). Quantitative prediction of line spread function measurements: Implications for channel bandwidth. *Vision Research*, **18**, 493-496.
53. Wilson, H. R., Levi, D., Maffei, L., Rovamo, J. and DeValois, R. (1990) The perception of form: retina to striate cortex. In L. Spillmann & J. S. Werner eds. *Visual Perception: The Neurophysiological Foundations.* San Diego: Academic Press.
54. Wilson, H.R., McFarlane, D.K., & Philips, G.C. (1983). Spatial frequency tuning of orientation selectivity units estimated by oblique masking. *Vision Research*, **23**, 873-882.
55. Wyszecki G. & Fiedler, G. H. (1971). New color-matching ellipses. *Journal of the Optical Society of America*, **61**, 1135-1152.
56. Wyszecki, G. & Stiles, W. S. (1982). *Color Science*. New York: Wiley.